Available online at www.sciencedirect.com
SCIENCE DIRECT®
Journal of Organometallic Chemistry 689 (2004) 2872–2879
Journal of Organometallic Chemistry
www.elsevier.com/locate/jorganchem

Synthesis, characterization and electrochemistry of ferrocenylselenolate bridged palladium(II) and platinum(II) complexes

Martin J. Brown, John F. Corrigan *

Department of Chemistry, The University of Western Ontario, London, Ont., Canada N6A 5B7

Received 3 February 2004; accepted 12 May 2004
Available online 21 July 2004

Abstract

The dimeric ferrocenyl-selenolate complexes of Pd and Pt, $[\{\mu\text{-}\eta^1\text{-}Fe(\eta^5\text{-}C_5H_4Se)_2\}M(P^nBu_3)]_2$ (M = Pd **2**, Pt **3**), and the monomeric ferrocenyl(bis-selenolate) complex of platinum, $[\{\eta^2\text{-}Fe(C_5H_4Se)_2\}Pt(P^nBu_3)_2]$ (**4**), have been prepared from 1,1′-bis(trimethylsilylseleno)ferrocene **1** and *trans*-$MCl_2(P^nBu_3)_2$ and *cis*-$PtCl_2(P^nBu_3)_2$, respectively. Complexes **2** and **3** contain two edge-sharing, square–planar metal centres forming a planar M_2Se_2 four-membered ring and exhibit two one-electron redox waves indicating electronic communication between the two Fe centers.

1. Introduction

The chemistry of transition metal–ferrocenylselenolate complexes has been increasing rapidly in recent years due to the structural diversity and various coordination modes exhibited by the selenolate ligand [1] and the inherent redox-active behavior of the iron centers of the ferrocenyl moiety [2]. The synthesis of transition metal–ferrocenylselenolates mirrors that developed for other metal–selenolate complexes, [1] including metathesis of an alkali metal–selenolate salt [3–8], cleavage of a Se–H bond via chalcogenolysis [9,10], and the oxidative addition of diferrocenyldiselenide [11–13]. The use of trimethylsilyl(ferrocenyl)selenides, which react with metals with a suitable leaving group such as a halide or an acetate ligand, also offers a direct entry into metal–ferrocenylselenolates. These reactions are driven by the formation of the thermodynamically stable, soluble silane (Eq. (1)) [14,15].

$$L_nM - X + RE - SiMe_3 \rightarrow L_nM - ER + X - SiMe_3 \quad (1)$$

Recently, the development and coordination chemistry of unsymmetrical 1,1′-disubstituted thiolato-ferrocenes with thioether and phosphine substituents have been reported [16–18]. These have been found to form bridging and monomeric and dimeric chelating structures with late metals. The incorporation of the ferrocenyl ligand allows for the determination of any electronic communication within the dimeric complexes [16]. As part of our development in the use of silylated–selenium complexes for promoting facile M–Se bond formation and our interest in electronic communication across a metal–chalcogenolate bridge, we report here on the synthesis and characterization of a set of ferrocenylselenolate–palladium and –platinum complexes from 1,1′-bis(trimethylsilylseleno)ferrocene **1**.

* Corresponding author. Tel.: +1-519-661-2111x86387; fax: +1-519-661-3022.
E-mail address: corrigan@uwo.ca (J.F. Corrigan).

0022-328X/$ - see front matter © 2004 Elsevier B.V. All rights reserved.
doi:10.1016/j.jorganchem.2004.05.044

2. Experimental

2.1. Materials and general procedures

All reactions were carried out under nitrogen using standard Schlenk and glovebox techniques, unless noted otherwise. Solvents were dried according to standard practices [19]. Chlorotrimethylsilane and *N*,*N*,*N*′,*N*′-tetramethylethylenediamine (TMEDA) were distilled prior to use. The starting materials P^nBu_3 [20], *trans*-$PdCl_2(P^nBu_3)_2$ [21], *trans*-$PtCl_2(P^nBu_3)_2$ [22], *cis*-$PtCl_2(P^nBu_3)_2$ [22], and 1,1′-bis(trimethylsilylseleno)ferrocene, **1** [14], were prepared and purified according to literature procedures.

2.2. [{μ-η¹-Fe(η⁵-$C_5H_4Se)_2$}$Pd(P^nBu_3)]_2$ (**2**)

To a solution of *trans*-$PdCl_2(P^nBu_3)_2$ (0.100 g, 0.172 mmol) in tetrahydrofuran (15 mL) was added Fe(η⁵-$C_5H_4SeSiMe_3)_2$ **1** (0.084 g, 0.172 mmol). The resulting red-brown solution was allowed to stir for two days. Removal of the solvent under reduced pressure left a dark red–brown solid. X-ray quality red plates were grown from the slow evaporation of tetrahydrofuran. Yield: 0.104 g (92.8%). Anal. Calc. for **2**: C, 40.61; H, 5.42. Found: C, 40.43; H, 5.90%. ^{1}H NMR $\delta(CDCl_3)$: 4.77 (broad s, 4H), 4.49 (virtual t, $^3J_{H-H}=1.5$ Hz, 4H), 4.05 (virtual t, $^3J_{H-H}=1.5$ Hz, 4H), 3.98 (virtual t, $^3J_{H-H}=1.4$ Hz, 4H), 1.69 (m, 12H), 1.34 (m, 24H), 0.88 (t, $^3J_{H-H}=7.0$ Hz, 18H). $^{31}P\{^1H\}$ NMR $\delta(CDCl_3)$: 7.36 (s). $^{77}Se\{^1H\}$ NMR $\delta(CDCl_3)$: 102.1 (s), −344.0 (d, $^2J_{P(trans)-Se}=177$ Hz). UV–Vis: $\lambda_{max}=470$ nm ($\varepsilon=2030$ $M^{-1}cm^{-1}$).

2.3. [{μ-η¹-Fe(η⁵-$C_5H_4Se)_2$}$Pt(P^nBu_3)]_2$ (**3**)

To a solution of *trans*-$PtCl_2(P^nBu_3)_2$ (0.050 g, 0.075 mmol) in tetrahydrofuran (15 mL) was added Fe(η⁵-$C_5H_4SeSiMe_3)_2$ **1** (0.036 g, 0.074 mmol). The resulting orange solution was heated to reflux and allowed to stir for two days. Removal of the solvent under reduced pressure left a light orange solid. X-ray quality orange plates were grown from the slow evaporation of diethyl ether. Yield: 0.020 g (33.3%). Anal. Calc. for **3**: C, 35.74; H, 4.77. Found: C, 35.72; H, 4.98%. ^{1}H NMR $\delta(CDCl_3)$: 4.71 (broad s, 4H), 4.45 (broad s, 4H), 4.11 (broad s, 4H), 4.02 (broad s, 4H), 1.68 (m, 12H), 1.55 (m, 12H), 1.34 (m, 12H), 0.88 (t, $^3J_{H-H}=7.0$ Hz, 18H). $^{31}P\{^1H\}$ NMR $\delta(CDCl_3)$: −0.92 (s, $^1J_{P-Pt}=3225$ Hz). $^{77}Se\{^1H\}$ NMR $\delta(CDCl_3)$: 56.6 (s), −305.1 (broad s). UV–Vis: $\lambda_{max}=431$ nm ($\varepsilon=1600$ $M^{-1}cm^{-1}$).

2.4. [{η²-Fe(η⁵-$C_5H_4Se)_2$}$Pt(P^nBu_3)_2$] (**4**)

To a solution of Fe(η⁵-$C_5H_4SeSiMe_3)_2$ **1** (0.055 g, 0.112 mmol) in tetrahydrofuran (15 mL) was added *cis*-$PtCl_2(P^nBu_3)_2$ (0.075 g, 0.112 mmol). The orange solution was allowed to stir for four days. Removal of the solvent under reduced pressure left a deep orange solid. X-ray quality orange rods were grown from the slow evaporation of chloroform. Yield: 0.076 g (63.3%). The product crystallizes with one equivalent of $CHCl_3$. Anal. Calc. for **4**·$CHCl_3$: C, 39.62; H, 5.98. Found: C, 39.41; H, 5.85%. ^{1}H NMR $\delta(CDCl_3)$: 4.10 (virtual t, $^3J_{H-H}=1.6$ Hz, 4H), 3.92 (virtual t, $^3J_{H-H}=1.6$ Hz, 4H), 1.47 (m, 12H), 1.40 (m, 12H), 1.31 (m, 12H), 0.88 (t, $^3J_{H-H}=7.0$ Hz, 18H). $^{31}P\{^1H\}$ NMR $\delta(CDCl_3)$: −0.39 (s, $^1J_{P-Pt}=2824$ Hz). $^{77}Se\{^1H\}$ NMR $\delta(CDCl_3)$: –36.9 (d of d, $^2J_{P(trans)-Se}=84$ Hz; $^2J_{P(cis)-Se}=17$ Hz; $^1J_{Pt-Se}=\sim100$ Hz,). $\lambda_{max}=416$ nm ($\varepsilon=1480$ $M^{-1}cm^{-1}$).

2.5. Crystallography

Crystals were mounted immersed in mineral oil and placed in a cold stream of N_2 during data collection. A single crystal suitable for X-ray analysis was mounted on a glass fibre. X-ray structural analyses were carried out on a Siemens SMART CCD (complex **2**), Enraf–Nonius Kappa CCD (complex **3**) and STÖE IPDS equipped with an imaging plate area detector and a rotating anode generator (complex **4**) single-crystal X-ray diffractometers using Mo Kα radiation. Crystal data, data collection parameters and analysis statistics for **2**–**4** are listed in Table 1. Data were corrected for Lorentz and polarization effects. The SHELXTL (G.M. Sheldrick, Madison, WI, v. 5.1) program package was used to solve and refine the structures. The weighting scheme employed was of the form $w=1/[\sigma^2(F_{obs}^2)+(\alpha P)^2+\beta P]$ (α,β = refined variables, $P=1/3\max(F_{obs}^2,\theta)+2/3F_c^2$).

2.6. Measurements

^{1}H (400.088 MHz) and $^{31}P\{^1H\}$ (161.957 MHz) NMR spectra were recorded at 20 °C on a Varian Mercury-400 spectrometer. The $^{77}Se\{^1H\}$ (76.220 MHz) NMR spectra were recorded at 20 °C on a Varian Inova-400 spectrometer. Chemical shifts are reported in ppm, and referenced to residual solvent for ^{1}H, external 85% H_3PO_4 for $^{31}P\{^1H\}$, external PhSeTMS used as a secondary reference ($\delta=82$ ppm relative to $SeMe_2$) for $^{77}Se\{^1H\}$. UV–Vis spectra were obtained using a Varian Cary 100 UV–Vis spectrophotometer using 1.00 cm matched quartz cells at room temperature, as solutions in tetrahydrofuran. Electrochemical measurements were obtained using a BAS 100W version 2.0 Electrochemical Analyzer potentiostat interfaced to a personal computer using BAS 100W version 2.0 software in a dichloromethane solution at room temperature containing 0.1 M $[NBu_4]BF_4$ electrolyte and ca. 2×10^{-3} M of the complex. Sweep rates were run between 50 and 500 mV/s. A three-electrode arrangement was used with a Pt working electrode, a 1 cm×1 cm Pt flag counter electrode and a

Table 1
Crystallographic data for complexes **2–4**

	2	**3**	**4**
Chemical formula	$C_{44}H_{70}Fe_2P_2Pd_2Se_4$	$C_{44}H_{70}Fe_2P_2Pt_2Se_4$	$C_{34}H_{62}FeP_2PtSe_2\cdot CHCl_3$
F_w	1301.28	1478.66	1061.00
Temperature (°C)	−50	−73	−83
Space group (no.)	*P2(1)/c* (14)	*P2(1)/c* (14)	*P2(1)/n* (14)
a (Å)	9.784(2)	9.7729(1)	14.003(4)
b (Å)	21.973(4)	21.9815(3)	18.159(5)
c (Å)	22.936(5)	22.8868(4)	16.418(7)
β (°)	94.691(4)	94.7110(10)	95.35(4)
V (Å^3)	4914 (2)	4900.0(1)	4157(2)
Z	4	4	4
ρ_{calc} (g cm^{-3})	1.759	2.004	1.695
μ (mm^{-1})	4.355	9.338	5.755
R indices [$(I)>2\sigma I$)][a]	$R_1=0.0585$	$R_1=0.0366$	$R_1=0.0519$
	$wR_2=0.0999$	$wR_2=0.0699$	$wR_2=0.1387$
R indices (all data)[a]	$R_1=0.1086$	$R_1=0.0779$	$R_1=0.0543$
	$wR_2=0.1187$	$wR_2=0.0808$	$wR_2=0.1412$

[a] $R_1 = \sum \|F_o\| - |F_c| / \sum |F_o| \cdot wR_2 = \sum[w(F_o^2 - F_c^2)^2 / \sum[wF_o^2]^2]^{1/2}$.

silver wire reference electrode. Potentials were referenced by adding a measured amount of ferrocene ($FeCp_2/FeCp_2^+$ $E^\circ = 0.528$ V in CH_2Cl_2 vs. aqueous SCE) [23]. This standard was also used to roughly confirm the number of electrons removed during the anodic oxidations. Elemental analyses were performed by Chemisar Laboratories Inc., (Guelph, Ont.).

3. Results and discussion

The reaction of 1,1′-bis(trimethylsilylseleno)ferrocene **1** with *trans*-$PdCl_2(P^nBu_3)_2$ affords the dimeric product $[\{\mu\text{-}\eta^1\text{-}Fe(\eta^5\text{-}C_5H_4Se)_2\}Pd(P^nBu_3)]_2$ **2** in 93% yield. Similarly, the reaction of **1** with *trans*-$PtCl_2(P^nBu_3)_2$ affords $[\{\mu\text{-}\eta^1\text{-}Fe(\eta^5\text{-}C_5H_4Se)_2\}Pt(P^nBu_3)]_2$ **3** in 33% yield. In both reactions, dimerization occurs with the loss of one phosphine ligand from each of the metal centers (Scheme 1). Similar reactions with excess tributylphosphine did not affect the amount of **2** and **3** that were formed. The monomeric platinum product $[\{\eta^2\text{-}Fe(\eta^5\text{-}C_5H_4Se)_2\}Pt(P^nBu_3)_2]$ **4** is obtained from the reaction of **1** with *cis*-$PtCl_2(P^nBu_3)_2$ in 63% yield (Scheme 2). Complex **4** is also formed in competition with the synthesis of **3**, presumably due to the *cis–trans* isomerization of $PtCl_2(P^nBu_3)_2$. Similarly, small amounts of **3** are isolated from the synthesis of **4**. Complexes **2–4** all show resolved maxima in the UV–Vis spectra between 400 and 475 nm, with molar absorptivity values on the order of 1.5×10^3 $M^{-1}cm^{-1}$, attributed to ferrocenyl d–d transitions.

The molecular structures, and the numbering of the atoms of $[\{\mu\text{-}\eta^1\text{-}Fe(\eta^5\text{-}C_5H_4Se)_2\}Pd(P^nBu_3)]_2$ **2** and $[\{\mu\text{-}\eta^1\text{-}Fe(\eta^5\text{-}C_5H_4Se)_2\}Pt(P^nBu_3)]_2$ **3** are illustrated in Figs. 1 and 2 and those for $[\{\eta^2\text{-}Fe(\eta^5\text{-}C_5H_4Se)_2\}Pt(P^nBu_3)_2]$ **4** are in Fig. 3. Selected bond angles and distances

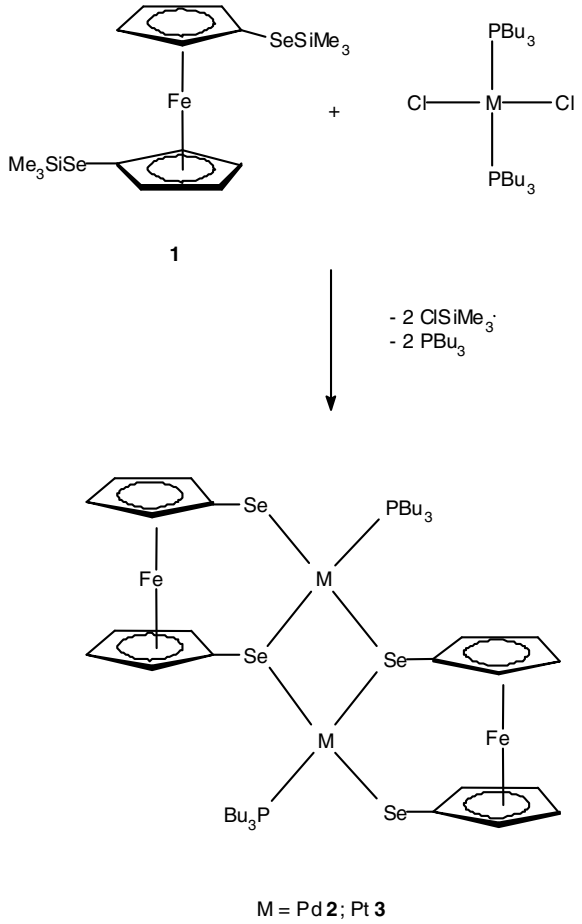

Scheme 1.

are summarized in Table 2. The dimeric complex **2** consists of two edge-sharing, slightly distorted square–planar palladium coordination centres. These are held

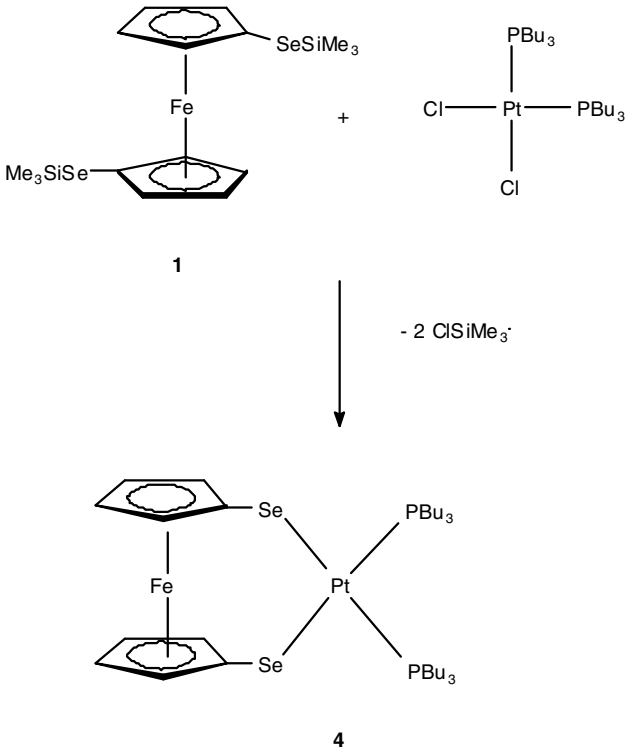

Scheme 2.

together by two μ_2-bridging selenolate ligands, one from each of the bis(seleno)ferrocenyl moieties forming a planar Pd_2–Se_2 ring. The Pd–Se bond lengths in **2** range between 2.450(1) and 2.457(1) Å for the terminal bonds and range between 2.459(1) Å and 2.492(1) Å for the bridging selenium centres. The bond lengths of the bridging atoms are comparable to those found in related Pd complexes with monodentate ligands such as

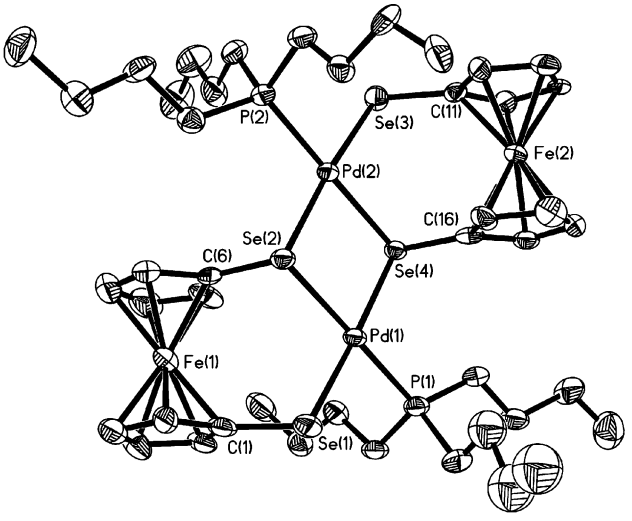

Fig. 1. Molecular structure of $[\{\mu\text{-}\eta^1\text{-}Fe(\eta^5\text{-}C_5H_4Se)_2\}Pd(PBu_3)]_2$ **2** showing the numbering scheme. Hydrogen atoms omitted for clarity. Thermal ellipsoids are drawn at the 40% probability level.

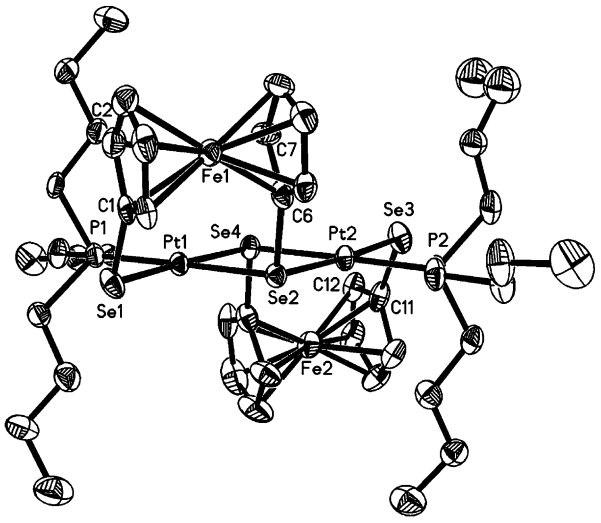

Fig. 2. Molecular structure of $[\{\mu\text{-}\eta^1\text{-}Fe(\eta^5\text{-}C_5H_4Se)_2\}Pt(PBu_3)]_2$ (**3**) illustrating the planar nature of the Pt_2Se_4 framework. Hydrogen atoms omitted for clarity. Thermal ellipsoids are drawn at the 40% probability level.

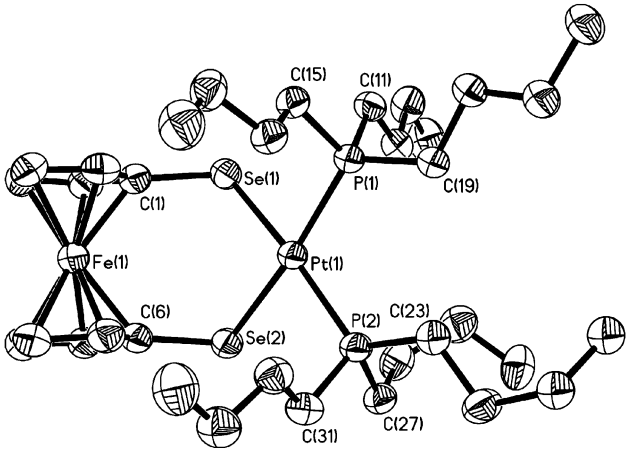

Fig. 3. Molecular structure of $[\{\eta^2\text{-}Fe(\eta^5\text{-}C_5H_4Se)_2\}Pt(PBu_3)_2]$ (**4**) showing the numbering scheme. Hydrogen atoms omitted for clarity. Thermal ellipsoids are drawn at the 40% probability level.

$[Pd_2\{Se(C_4H_3S)\}_4(PPh_3)_2]$ (2.4657(12)–2.4661(11) Å) [24], $[Pd_2(SePh)_4(PPh_3)_2]$ (2.463(1)–2.494(1) Å), [25] and $[Pd_2\{SeC(CH_2)_6{=}C(CH_2)Se\}_2(PPh_3)_2]$ (2.413(4)–2.489(4) Å) [26]. This $M_2X_2(\mu\text{-}ER)_2(PR'_3)_2$ type of bridging structure is quite common for palladium and platinum complexes due to the high polarizability of the heavier chalcogen centres.

The dimeric complex **3** has the same general structural features as its lighter congener **2** with a planar Pt_2Se_2 central ring as well as two ferrocenyl and two phosphine groups. The Pt–Se bond lengths range between 2.4491(6) and 2.4537(7) Å for the terminally bonded ligands and between 2.4499(6) and 2.4889(6) Å for the bridging groups. Again, the bond lengths

Table 2
Selected bond lengths (Å) and bond angles (°) for **2**–**4**

2			
Pd(1)–P(1)	2.272(3)	Pd(2)–P(2)	2.274(3)
Pd(1)–Se(1)	2.457(1)	Pd(2)–Se(3)	2.450(1)
Pd(1)–Se(4)	2.459(1)	Pd(2)–Se(2)	2.472(1)
Pd(1)–Se(2)	2.492(1)	Pd(2)–Se(4)	2.481(1)
P(1)–Pd(1)–Se(1)	87.39(8)	P(2)–Pd(2)–Se(3)	87.46(8)
P(1)–Pd(1)–Se(4)	96.50(8)	P(2)–Pd(2)–Se(2)	97.74(8)
Se(1)–Pd(1)–Se(4)	175.93(5)	Se(3)–Pd(2)–Se(2)	174.77(5)
P(1)–Pd(1)–Se(2)	179.31(9)	P(2)–Pd(2)–Se(4)	177.78(9)
Se(1)–Pd(1)–Se(2)	91.93(5)	Se(3)–Pd(2)–Se(4)	90.65(5)
Se(4)–Pd(1)–Se(2)	84.18(4)	Se(2)–Pd(2)–Se(4)	84.16(4)
3			
Pt(1)–P(1)	2.256(2)	Pt(2)–P(2)	2.255(2)
Pt(1)–Se(1)	2.4491(6)	Pt(2)–Se(2)	2.4499(6)
Pt(1)–Se(4)	2.4600(6)	Pt(2)–Se(3)	2.4537(7)
Pt(1)–Se(2)	2.4771(6)	Pt(2)–Se(4)	2.4889(6)
P(1)–Pt(1)–Se(1)	88.69(4)	P(2)–Pt(2)–Se(2)	96.78(4)
P(1)–Pt(1)–Se(4)	98.03(4)	P(2)–Pt(2)–Se(3)	88.60(4)
Se(1)–Pt(1)–Se(4)	173.28(2)	Se(2)–Pt(2)–Se(3)	174.35(2)
P(1)–Pt(1)–Se(2)	178.76(4)	P(2)–Pt(2)–Se(4)	179.28(5)
Se(1)–Pt(1)–Se(2)	90.21(2)	Se(2)–Pt(2)–Se(4)	83.034(2)
Se(4)–Pt(1)–Se(2)	83.071(2)	Se(3)–Pt(2)–Se(4)	91.60(2)
4			
Pt(1)–P(1)	2.290(1)	Pt(1)–Se(1)	2.4855(9)
Pt(1)–P(2)	2.290(2)	Pt(1)–Se(2)	2.4855(8)
P(1)–Pt(1)–P(2)	104.93(6)	P(1)–Pt(1)–Se(2)	171.20(4)
P(1)–Pt(1)–Se(1)	83.57(5)	P(2)–Pt(1)–Se(2)	83.25(4)
P(2)–Pt(1)–Se(1)	169.15(4)	Se(1)–Pt(1)–Se(2)	87.93(3)

of the μ_2-Se centers are comparable to those found in the related complex $[Pt_2\{Se(C_4H_3S)\}_4(PPh_3)_2]$ (2.4461(10)–2.4715(10) Å) [24].

This planar arrangement of the M_2E_2 central four-membered ring observed in **2** and **3**. (M = Pd, Pt; E = Se, Te) is a common one for $L(RE)M(\mu\text{-}ER)_2M(ER)L$ complexes [24–26]. A 'hinged' arrangement is also observed for $L(X)M(\mu\text{-}ER)_2M(X)L$ (E = S, Se, Te; X = halide, ER, etc) complexes, with non-coplanar four-membered rings [27]. The two structural types have been rationalized on the delicate balance of conformational preferences of the bridging groups, the presence of weak metal–metal bonding in the bent structures and the steric requirements of the ligands around the two metals [27].

The tendency for chalcogenolate complexes is to adopt a bridging geometry rather then the terminal geometry favoured by chalcogenoether complexes [17]. This has been demonstrated by the work of Long and co-workers [18a] where an asymmetric phosphine- and thiolate-substituted ferrocenediyl ligand, $Fe(\eta^5\text{-}C_5H_4SH)(\eta^5\text{-}C_5H_4PPh_2)$, forms the ('bent') dimeric complex with palladium incorporating a bridging thiolate moiety. When a similar asymmetric phosphine- and thioether-substituted ferrocenediyl ligand, $Fe(\eta^5\text{-}C_5H_4SMe)(\eta^5\text{-}C_5H_4PPh_2)$, was used, either a chelating or linear complex, the latter with coordination to the metal exclusively through the phosphine, was observed [18b].

The monomeric complex **4** can be prepared in good yields from *cis*-$PtCl_2(P^nBu_3)_2$ (Scheme 2) and is also formed in minor amounts from *trans*-$PtCl_2(P^nBu_3)_2$ due to the slow isomerization of *trans*-$PtCl_2(P^nBu_3)_2$ to *cis*-$PtCl_2(P^nBu_3)_2$. Complex **4** contains one chelating ferrocenyl(bis)selenolate ligand and two phosphine groups in a *cis* orientation, a related complex having been prepared from $Fe(C_5H_4SeH)_2$ and $Pt(PPh_3)_4$ [28]. The two Pt–Se bond lengths are equivalent, 2.4855(8) and 2.4855(9) Å, and these lengths are very close to the equivalent bonds in **3**, 2.4771(6) and 2.4889(6) Å. As is observed in **2** and **3**, there is a distorted square–planar geometry around the platinum centre. The P(1)–Pt(1)–P(2) angle is 104.93(6)° whereas the Se(1)–Pt(1)–Se(2) angle is only 87.93(3)°. These values contrast with those observed in the recently reported *cis*-$(Ph_3P)_2Pt(SePh)_2$, 97.40(2)° and 95.10(1)°, respectively [29]. Ferrocenylthiolate complexes $[\{\eta^2\text{-}Fe(\eta^5\text{-}C_5H_4S)_2\}M(Ph_2PC_2H_4PPh_2)]$ (M = Pd, Pt) have been characterized crystallographically [30]. These also display distorted square–planar geometry around the palladium and platinum centers however unlike in **4**, they both display a staggered arrangement of the cyclopentadienyl rings [30].

The ^{1}H NMR spectrum of **2** has, in addition to four resonances for P^{n}Bu$_3$, four resonances for the two types of non-equivalent cyclopentadienyl rings protons at $\delta = 4.77$, 4.49, 4.05 and 3.98 ppm. The three higher field peaks are resolved as virtual triplets with $^3J_{H-H}$ of 1.5 Hz. These are at comparable shifts and have similar coupling constants to the starting material **1**. The ^{1}H NMR spectrum of **3** also has four resonances for the cyclopentadienyl-ring protons at 4.71, 4.45, 4.11 and 4.02 ppm, for which no resolved $^3J_{H-H}$ is observed. The ^{1}H NMR spectrum of **4** has two resonances for the protons on the equivalent cyclopentadienyl rings at 4.10 and 3.92 ppm and are resolved as virtual triplets with coupling constants of 1.6 Hz. The ^{31}P{^{1}H} NMR spectrum of **2** consists of a single peak at 7.36 ppm and the spectra of **3** and **4** each consist of a central peak at −0.92 and −0.39 ppm, respectively, with the expected satellites from coupling to ^{195}Pt ($^1J_{PtP} = 2824$ Hz).

The ^{77}Se{^{1}H} NMR spectra for **2** and **3** each contain two resonances, consisting of a singlet at +102 ppm and a doublet at −344 ppm for **2**, and a broad singlet at +56 ppm and a broad peak at −305 ppm for **3**. The low field shifts are close to that observed for **1** (9.7 ppm). The low field shift for **2** is assigned to the terminally bonded Se atoms that are *cis* to the phosphine groups, and the higher field doublet ($^2J_{PSe} = 177$ Hz) to the bridging Se atoms that are *trans* to the P^{n}Bu$_3$ ligands [24]. As in **2**, the low-field shift for **3** at +56 ppm is assigned to the terminal Se and the high-field shift at −305 ppm is assigned to the bridging Se atoms. The P–Se coupling for **3** was not resolved.

The ^{77}Se{^{1}H} NMR spectrum for **4** has asingle resonance at −36.9 ppm. A splitting pattern is observed in which coupling to ^{195}Pt ($^1J_{Pt-Se} \sim 100$ Hz), and to both *trans* and *cis* phosphine groups ($^2J_{P(trans)-Se} = 84$ Hz; $^2J_{P(cis)-Se} = 12$ Hz) are resolved. These values are comparable to those observed in related $P_2Pt(SeR)_2$ complexes [31–33].

3.1. Electrochemistry

Cyclic voltammetry was used to investigate the electronic communication between the two iron centres in complexes **2** and **3**. The cyclic voltammograms are shown in Figs. 4 and 5. Two quasi-reversible, one-electron anodic oxidation waves are observed in the CV of **2** and **3** at $E_{1/2}(1) = 398$ mV and $E_{1/2}(2) = 560$ mV, and at $E_{1/2}(1) = 430$ mV and $E_{1/2}(2) = 565$ mV, respectively. The difference between the first and second ferrocenyl oxidation, ΔE, is 162 mV for **2** and 135 mV for **3** ($\Delta E = E_{1/2}(2) - E_{1/2}(1)$), suggesting moderate electronic communication [34]. The starting material **1**, bis(trimethylsilylseleno)ferrocene, displays an irreversible oxidation wave at 375 mV [14], which is similar to the first oxidation values observed in both **2** and **3**. We see that the incorporation of platinum decreases the extent of

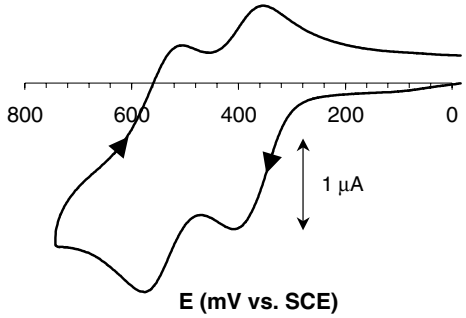

Fig. 4. Cyclic voltammogram of [{μ-η^1-Fe(η^5-$C_5H_4Se)_2$}Pd(PBu_3)]$_2$ **2** (2.15 mM) in dichloromethane/0.2 M N(^{n}Bu)$_4$BF$_4$ with a 200 mV/s scan rate using a Pt wire working electrode, a Pt flag counter electrode and a Ag wire pseudo-reference electrode.

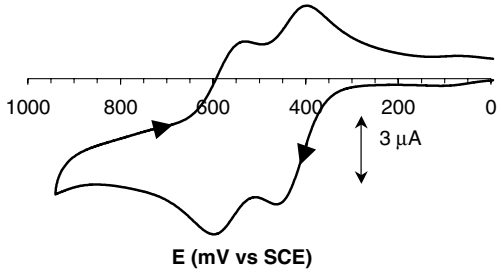

Fig. 5. Cyclic voltammogram of [{μ-η^1-Fe(η^5-$C_5H_4Se)_2$}Pt(PBu_3)]$_2$ **3** (2.03 mM) in dichloromethane/0.2 M N(^{n}Bu)$_4$BF$_4$ with a 200 mV/s scan rate using a Pt wire working electrode, a Pt flag counter electrode and a Ag wire pseudo-reference electrode.

electronic interaction between the two iron centres relative to the palladium complexes, similar to observations with palladium and platinum ferrocenylthiolates [16].

Two one-electron anodic oxidation waves are also observed for [{η^2-Fe(η^5-$C_5H_4Se)_2$}Pt(P^{n}Bu$_3$)$_2$] **4** and the cyclic voltammogram is shown in Fig. 6. With only one Fe^{II} centre, the first wave at lower potential ($E_{1/2}(1) = 194$ mV) is easily assigned to the oxidation of Fe^{II} to Fe^{III} based upon similar values reported for related complexes **2** and **3**. The second wave, of equal amplitude, at higher potential ($E_{1/2}(2) = 739$ mV) can be assigned to the one electron oxidation of one of the

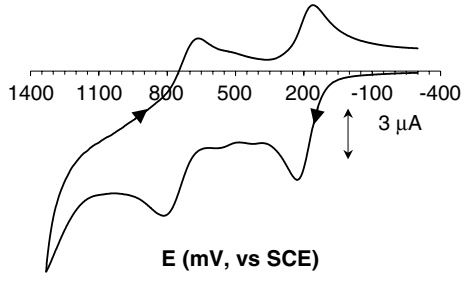

Fig. 6. Cyclic voltammogram of [{η^2-Fe(η^5-$C_5H_4Se)_2$}Pt(PBu_3)$_2$] (**4**) (2.26 mM) in dichloromethane/0.2 M N(^{n}Bu)$_4$BF$_4$ with a 200 mV/s scan rate using a Pt wire working electrode, a Pt flag counter electrode and a Ag wire pseudo-reference electrode.

selenium atoms. Similar behaviour has been reported for monosubstituted ferrocenyl alkyl selenides, such as $[Fe(\eta^5\text{-}C_5H_5)(\eta^5\text{-}C_5H_4SeR)]$, in which two oxidation waves were observed [35]. The first oxidation wave was assigned to the Fe centre and the second oxidation wave, occurring between 770 and 970 mV vs. SCE, was assigned to the oxidation of the selenium centre. Similarly. theoretical and electrochemical studies on 1,1′-ferrocene dichalcogenido complexes of Rh and Ir suggest that the chalcogen centres contribute greatly to the orbitals involved in the electron removal processes [36].

4. Conclusions

A set of monomeric and dimeric ferrocenyl-containing palladium– and platinum–selenolate complexes has been prepared. The dimeric complexes contain two edge-joined square–planar metal centres forming a planar M_2Se_2 four-membered ring. The monomeric complex contains one square–planar metal centre. Electrochemical studies have demonstrated that electronic communication occurs between the two Fe centres in the dimeric complexes. The use of these same metal–chalcogen bond-forming strategies to incorporate different metal centres with a range of different phosphine ligands may lead to further interesting monomeric, dimeric and possibly oligomeric materials.

5. Supplementary material

Crystallographic data for the structural analysis have been deposited with the Cambridge Crystallographic Data Centre, CCDC No. 220285-220287 for **2**–**4**. Copies of this information may be obtained free of charge from The Director, CCDC, 12 Union Road, Cambridge CB2 1EZ, UK fax: (int.code) +44(1223) 336-033 or e-mail: deposit@ccdc.cam.ac.uk.

Acknowledgement

We thank the Natural Sciences and Engineering Research Council of Canada, the Government of Ontario's PREA program and The University of Western Ontario's ADF program for supporting this research. We thank Prof. Hilary Jenkins (St. Mary's University) and Dr. Michael Jennings (UWO) for X-ray data collection and Dr. Chris Kirby for his assistance with the ^{77}Se NMR measurements. Prof. Dieter Fenske (Universität Karlsruhe) and Prof. Mark S. Workentin (UWO) are gratefully acknowledged for the use of their X-ray diffractometer and electrochemical equipment, respectively.

References

[1] (a) M.W. Degroot, J.F. Corrigan, in: M. Fujita, A. Powell, C. Creutz (Eds.), Comprehensive Coordination Chemistry II, vol. 7, Pergamon, 2004, p. 57;
(b) J. Arnold, Prog. Inorg. Chem. 43 (1995) 353.
[2] M. Herberhold, in: A. Togni, T. Hayashi (Eds.), Ferrocenes: Homogeneous Catalysis, Organic Synthesis, Materials Science, Wiley, New York, 1995 (Chapter 5).
[3] M. Herberhold, G.-X. Jin, A.L. Rheingold, Z. Anorg. Allg. Chem. 628 (2002) 1985.
[4] M. Herberhold, G.-X. Jin, W. Milius, J. Organomet. Chem. 512 (1996) 111.
[5] M. Herberhold, C. Doernhoefer, A. Scholz, G.-X. Jin, Phosphorus, Sulfur, Silicon Rel. Elem. 64 (1992) 161.
[6] M. Herberhold, G.-X. Jin, I. Trukenbrod, W. Milius, Z. Anorg. Allg. Chem. 622 (1996) 724.
[7] M. Herberhold, M. Schrepfermann, A.L. Rheingold, J. Organomet. Chem. 394 (1990) 113.
[8] M. Heberhold, G.-X. Jin, A, L, Rheingold, G.F. Sheats, Z. Naturforsch. B 47 (1992) 1091.
[9] R. Broussier, Y. Gobet, R. Amardeil, A. Da Rold, M.M. Kubicki, B. Gautheron, J. Organomet. Chem. 445 (1993) C4.
[10] S. Akabori, T. Kumagai, T. Shirahige, S. Sato, K. Kawazoe, C. Tamura, M. Sato, Organometallics 6 (1987) 526.
[11] M. Herberhold, J. Peukert, M. Kruger, D. Daschner, W. Milius, Z. Anorg. Allg. Chem. 626 (2000) 1289.
[12] H. Matsuzaka, J.-P. Qu, T. Ogino, M. Nishio, Y. Nishibayashi, Y. Ishii, S. Uemura, M. Hidai, J. Chem. Soc., Dalton Trans. (1996) 4307.
[13] R. Kaur, H.B. Singh, R.P. Patel, S.K. Kulshreshtha, J. Chem. Soc., Dalton Trans. (1996) 461.
[14] A.I. Wallbank, J.F. Corrigan, Chem. Commun. (2001) 377.
[15] T.P. Lebold, D.L.B. Stringle, M.S. Workentin, J.F. Corrigan, Chem. Commun. (2003) 1398.
[16] V.C. Gibson, N.J. Long, C.K. Williams, M. Fontani, P. Zanello, Dalton Trans. (2003) 3599.
[17] V.C. Gibson, N.J. Long, R.J. Long, A.J.P. White, C.K. Williams, D.J. Williams, Dalton Trans. (2000) 2359.
[18] (a) V.C. Gibson, N.J. Long, A.J.P. White, C.K. Williams, D.J. Williams, Organometallics 21 (2002) 770;
(b) V.C. Gibson, N.J. Long, A.J.P. White, C.K. Williams, D.J. Williams, M. Fontani, P. Zanello, Dalton Trans. (2002) 3280.
[19] R.J. Errington, Advanced Practical Inorganic and Metalorganic Chemistry, Blickie Academic and Professional, London, 1997.
[20] G.B. Kauffman, L.A. Teter, Inorg. Synth. 6 (1960) 87.
[21] F.R. Hartley, The Chemistry of Palladium and Platinum, Applied Science Publishers Ltd., London, 1973 p. 458.
[22] G.B. Kauffman, L.A. Teter, Inorg. Synth. 9 (1963) 24.
[23] P. Hapiot, L.D. Kispert, V.V. Konovalov, J.-M. Savéant, J. Am. Chem. Soc. 123 (2001) 6669.
[24] R. Oilunkaniemi, R.S. Laitinen, M. Ahlgrén, J. Organomet. Chem. 587 (1999) 200.
[25] R. Oilunkaniemi, R.S. Laitinen, M. Ahlgrén, J. Organomet. Chem. 623 (2001) 168.
[26] S. Ford, P.K. Khanna, C.P. Morley, M. Di Vaira, J. Chem. Soc., Dalton Trans. (1999) 791.
[27] G. Aullón, G. Ujaque, A. Lledós, S. Alvarez, Chem. Eur. J. 5 (1999) 1391 and references therein.
[28] S. Akabori, T. Kumagai, T. Shirahige, Organometallics 6 (1987) 526.
[29] M.S. Hannu, R. Oilunkaniemi, R.S. Laitinen, M. Ahlgén, Inorg. Chem. Commun. 3 (2000) 397.
[30] S. Takemoto, S. Kuwata, Y. Nishibayashi, M. Hidai, Inorg. Chem. 37 (1998) 6428.

[31] (a) P.K. Khanna, C.P. Morley, M.B. Hursthouse, K.M.A. Malik, O.W. Howarth, Heteroatom Chem. 6 (1995) 519;
(b) S. Ford, M.R. Lewtas, C.P. Morley, M. Di Vaira, Eur. J. Inorg. Chem. (2000) 933.
[32] S. Narayan, V.K. Jain, B. Varghese, J. Chem. Soc., Dalton Trans. (1998) 2359.
[33] A. Singhal, V.K. Jain, B. Varghese, E.R.T. Tiekink, Inorg. Chim. Acta 285 (1999) 190.
[34] D. Osella, L. Milone, C. Nervi, M. Ravera, J. Organomet. Chem. 488 (1995) 1.
[35] M.R. Burgess, C.P. Morley, J. Organomet. Chem. 623 (2001) 101.
[36] P. Zanello, M. Casarin, L. Pardi, M. Heberhold, G.-X. Jin, J. Organomet. Chem. 503 (1995) 243.